Citation: Yixuan Fu, Yi Zhu, Zhou Zhao, et al. Feasibility and reliability study on GH4169/Cast iron bimetallic exhaust valves. *Journal of Harbin Institute of Technology (New Series)*. DOI:10.11916/j.issn.1005-9113.25052

Feasibility and Reliability Study on GH4169/Cast Iron Bimetallic Exhaust Valves

*Yixuan Fu, Yi Zhu, Zhou Zhao, Kaiheng Sun and Jinxiang Liu**

(*School of Mechanical Engineering, Beijing Institute of Technology, Beijing 100081, China*)

Abstract: In order to extend the service life of exhaust valves in high power density diesel engines, bimetal can be used for exhaust valves. A GH4169/cast iron bimetal was made with Laser Powder Bed Fusion (LPBF) tech, and the feasibility and dependability under exhaust valve operating conditions were thoroughly examined. This study determined the temperature distribution and stress distribution of the exhaust valve under service conditions using steady-state thermal analysis and dynamic mechanical analysis. The reliability of GH4169/cast iron bimetal applied to exhaust valves was evaluated through tensile and fatigue testing. From research findings, it can be seen that increasing the ratio of cast iron in bimetallic exhaust valves improves the overall heat conduction performance of the exhaust valve. There is significant stress concentration in the geometric transition area of the exhaust valve, and the stress can reach 166.5 MPa when combustion occurs. From the experimental data, we can see that when porosity is less than 2.68%, fatigue mainly depends on the properties of the cast iron rather than on porosity. The tensile strength of the GH4169/cast iron bimetal is 478.51 MPa at 400 ℃, 490.40 MPa at 500 ℃, and 462.24 MPa at 600 ℃. All corresponding fatigue strength values are over 135 MPa, far above the working stress of the exhaust valve stem. To take into account the exhaust valves' thermo-mechanical behavior as well as the bimetal's properties at higher temperatures, placing the bimetal interface on the stem would work. When the interface is in position 2, the bimetal offers the best balance of performance and cost.

Keywords: bimetallic exhaust valves; dynamic behavior; temperature distribution; feasibility assessment

CLC number: TK05 **Document code**: A **Article ID**: 1005-9113(2026)00-0000-12

0 Introduction

The combustion chamber components of a diesel engine are subject to very extreme working conditions. As an important seal part, the exhaust valve operates at temperatures over 700°C, and it is continuously in contact with corrosive high-temperature gases during each working cycle, and is frequently impacted by opening and closing during the working process, thus wearing[1-2]. Diesel engine power density keeps going up, so exhaust valve performance and dependability get more challenging. In extreme service circumstances, exhaust valve materials must meet many interrelated performance requirements simultaneously. The valve head should have high-temperature resistance, corrosion resistance, and oxidation[3-5]. On the contrary, the exhaust valve stem needs to have good wear resistance, mechanical strength, and thermal conductivity to improve the overall heat dissipation performance of the exhaust valve[6]. Single material exhaust valves cannot be achieved with these complex and varied requirements at the same time, and the commonly used austenitic and martensitic stainless steels have reached their limits, making it difficult to meet the growing demand for reliability.

Bimetallic structures combine the merits of different materials and balance between performance and economy. Thus, they are a perfect choice for exhaust valves. The previous research[7-8] has produced bimetallic exhaust valves with friction welding, but due to some flaws, such as slag inclusion and misalignment, formed during the welding process, the quality of dissimilar-material joints[9] deteriorates, and these are one of the major

Received 2025-11-29.

* Corresponding author. Jinxiang Liu, Ph.D, professor. Email: Liujx@bit.edu.cn.

causes for premature failure of the exhaust valves[10]. Compared to traditional welding, LPBF (Laser Powder Bed Fusion) provides better metal fusion without porosities, cracks, and other defects[11]. Furthermore, it can be used for high-quality manufacturing, strong metallurgical bonding of dissimilar materials, and compositional gradient transition to reduce thermal expansion mismatch between the two materials.

GH4169 provides high strength at elevated temperatures and excellent resistance to oxidation and hot corrosion[12]. It has been increasingly applied to exhaust valves[13], while cast iron offers advantages of wear resistance, machinability, and low cost[14]. Applying GH4169/cast iron bimetallic exhaust valves fabricated by LPBF can achieve an optimal balance among performance, cost, and manufacturability while enhancing long-term service reliability. The overall service life of GH4169/cast iron bimetallic exhaust valves is governed mainly by the structural integrity of the bimetallic interface and the axial distribution of the two materials. Interfacial defects determine bonding quality, while the position of the interface directly influences the exhaust valve's temperature field and the compatibility of thermal expansion between materials, collectively affecting stress states and safety margins under thermo-mechanical loading. Optimizing the interface position, therefore, provides the most effective compromise between high-temperature load-bearing capacity and economic efficiency.

Finite Element Modeling (FEM) is widely applied for designing and checking the failure of the exhaust valve. By numerically simulating the temperature field, stress distribution, and dynamic responses of exhaust valves under common operating scenarios, FEM can quantitatively assess the service performance of exhaust valves under complex thermo-mechanical loads. These loads include high-temperature gas impact, inertial force when the valve opens and closes, and contact stress between the valve seat and the valve. Previous work suggests that there are high thermal and mechanical stresses in the transition zone from the valve head to the valve neck because of the geometric discontinuity and the concentration of the temperature gradient[15-16]. Also, transients caused by valve closure are significant contributors to low-cycle fatigue damage[17]. FEM would provide superior insight with respect to the effects of where one positions interfaces, where one places the materials, and the differences in the thermo-physics on how that translates into overall mechanical and thermal-mechanical performance for the bimetallic exhaust valve. The simulated temperature and stress fields can provide a scientific basis for the selection of materials, interface optimization, and durability evaluation to achieve a balance of high-temperature bearing capacity under weight restrictions and economic feasibility. Therefore, FEM helps develop exhaust valves that are structurally stronger and more reliable in the long term.

To determine the optimal interface position between two metals of bimetallic exhaust valves, which can make a good balance between high temperature performance and economy efficiency, this study conducted tensile and fatigue tests on bimetallic specimens. Exhaust valve thermal characteristics and closing dynamics were observed at different interface positions. A steady-state heat transfer model is used to simulate the exhaust valve temperature distribution under service conditions. A dynamic model was used to analyze the valve seat forces and their stress equivalent. Complementary LPBF process trials and tensile/fatigue testing of the interfaces under varied porosity conditions. The high-temperature tensile strength of the bimetallic material fabricated under optimal conditions was determined, enabling evaluation of the operational reliability of the bimetallic exhaust valve. This research identifies the optimal interface window for GH4169/cast iron bimetallic exhaust valves to ensure high reliability and low service costs. It also provides the necessary information for their engineering application.

1 Methodology

1.1 Experimental Methods

1.1.1 Preparation of bimetal

GH4169 was fabricated on a cast iron substrate using LPBF, forming a GH4169/cast iron bimetal. The layer-by-layer building process in LPBF is illustrated in Fig.1. The LPBF-fabricated GH4169 deposit is a cylindrical specimen measuring 12 mm in diameter and 35 mm in height, which was used for subsequent tensile and fatigue tests.

The GH4169 powder had a mean particle size of 34 μm; the layer thickness was 30 μm, and the

powder-bed packing density was approximately 46%. The laser spot diameter was 70 μm during manufacturing, and the cast iron substrate was preheated to 200 ℃. Based on our previous work[18], an L16 orthogonal array with three factors at four levels was employed to conduct 16 process trials; for each trial, the relative density of the fabricated GH4169 was measured using the Archimedes immersion method. Porosity was calculated as 100% − relative density (%). From the 16 parameter sets, four GH4169/cast iron bimetal specimens—with distinct porosities in the GH4169 portion—were selected for tensile and fatigue testing to assess reliability; the corresponding process parameter combinations are summarized in Table 1.

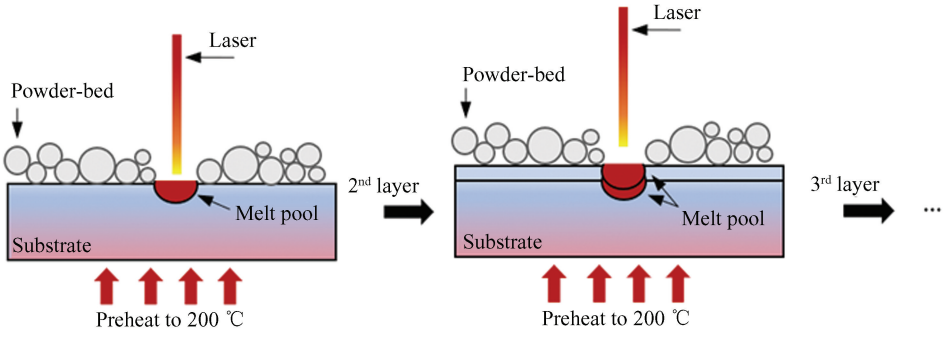

Fig.1 The layer-by-layer building process in LPBF

Table 1 Parameter combinations

Process scheme	Laser power (W)	Laser scanning speed (mm/s)	Scanning hatch (mm)	Porosity (%)
1	100	1050	0.13	12.05
2	100	900	0.10	4.24
3	200	1050	0.16	2.68
4	100	750	0.07	0.27

1.1.2 Tensile and fatigue testing

Monotonic tensile and cyclic fatigue tests were conducted to assess the reliability of GH4169/cast iron bimetal for exhaust valve applications. Both tests employed standard cylindrical specimens, as shown in Fig.2. The gauge section had a diameter of 5 mm and a length of 30 mm, and the grip ends had a diameter of 10 mm.

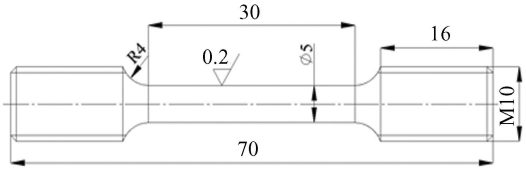

Fig. 2 Standard cylindrical specimens(unit:mm)

The MTS 809 servo-hydraulic testing system (as shown in Fig. 3) performed strain- or stress-controlled loading for the tensile and fatigue experiments. A box-type resistance furnace integrated with the frame provided specimen heating; K-type thermocouples monitored the furnace environment, and an additional thermocouple measured the specimen temperature in real time. For the tensile tests, according to GB/T 228.1−2021, strain-controlled loading was applied at a rate of 2.5×10^{-4} s^{-1} until fracture, yielding the bimetal stress-strain response.

Fig.3 The MTS 809 servo-hydraulic testing system

For the fatigue tests, in accordance with GB/T 3075−2008, axial tension-compression cyclic loading

with a sinusoidal waveform was applied, with a maximum nominal stress of 250 MPa, a load ratio R = 0.1, and a frequency of 5 Hz. Tests were performed at room temperature (≈ 25 ℃) and at elevated temperature (250 ℃) using the box furnace, with environmental temperature stability maintained within ±5 ℃; the specimen temperature was continuously monitored, and the cycles to fatigue failure were recorded to evaluate the fatigue life and fracture mechanisms of GH4169/cast iron bimetal at different porosities.

1.2 Simulation Method

1.2.1 Model of the exhaust valve

A V-type 12-cylinder engine exhaust valve was selected as the research object. A single-exhaust valve assembly model was established to analyze the thermal and dynamic characteristics of the exhaust valve under service conditions. The single-exhaust valve assembly consists of the camshaft, exhaust valve spring seat, exhaust valve spring, exhaust valve guide, and exhaust valve seat, as illustrated in Fig. 4(a); the exhaust valve spring was represented using connector elements (as shown by the red line in Fig. 4(a)). Tetrahedral elements were employed to mesh the components of the single-exhaust valve system, as shown in Fig. 4(b). The cam was meshed with an element size of 0.5 mm to ensure the accuracy of the cam profile, while the remaining components were meshed with an element size of 1 mm. The thermal and mechanical simulations of the single-exhaust valve assembly were carried out using Abaqus software.

The materials assigned to the components of the single-exhaust valve assembly mainly include austenitic stainless steel (21-4N), cast iron, and GH4169; their physical properties are listed in Table 2. The cam and exhaust valve spring seat were modeled with the material properties of alloy steel. The exhaust valve guide and seat were assigned the material properties of cast iron. The exhaust valve was composed of two materials: GH4169 for the valve head and cast iron for the valve stem. The proportions of GH4169 and cast iron within the exhaust valve were determined by the interface location. As illustrated in Fig. 5, four different interface positions were designed in the simulation, and the material of the exhaust valve was assigned accordingly based on each interface position.

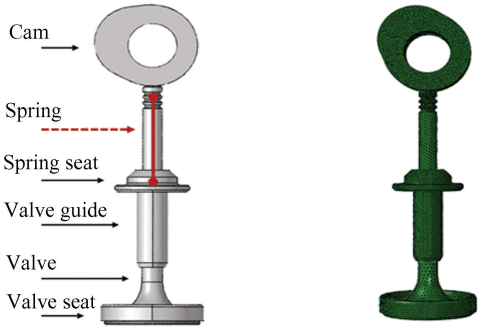

Fig. 4 Single-exhaust valve assembly model

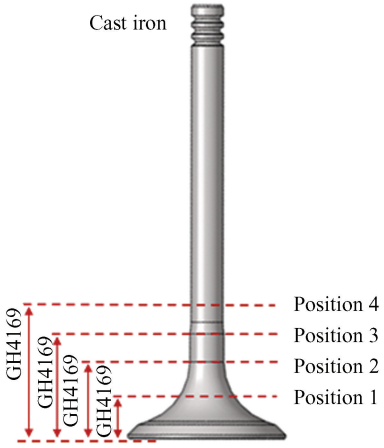

Fig. 5 Interface position of the bimetallic exhaust valve

Table 2 Material physical properties (room temperature)

Material	Density (kg/m^3)	Elastic modulus (GPa)	Yield strength (MPa)	Tensile strength (MPa)	Coefficient of thermal expansion ($\times10^{-6}$)	Thermal conductivity (W/(m·k))
21-4N	7900	212	580	950	14.5	14.5
Cast iron	7000	135	295	350	11.0	43.0
GH4169	8240	204	1100	1350	13.0	13.4

1.2.2 Boundary conditions

Based on the loading characteristics of the exhaust valve, the thermal conditions during seating can be divided into 5 regions, as presented in Fig.6: (1) Exhaust valve head bottom region (A): During exhaust valve opening, this area is exposed to high-speed, high-temperature gas impingement; during seating, it becomes part of the combustion chamber and remains in continuous contact with hot gases, thereby experiencing concentrated thermal loading.

(2) Exhaust valve seat face/conical surface (*B*): During opening, it is impinged by hot exhaust gas; during seating, it is in tight contact with the exhaust valve seat insert. Heat is transferred from the exhaust valve through this contact into the seat insert and dissipated via the cylinder head and cooling water jacket. (3) Exhaust valve neck (*C*): With a small cross-sectional area, the neck is directly scoured by hot gases. During opening, the local gas velocity rises sharply at this section, significantly increasing the convective heat transfer coefficient and raising the local temperature. (4) Exhaust valve stem (*D*): During opening, part of the stem is exposed to the exhaust port; during seating, it enters the exhaust valve guide, where heat is dissipated mainly through conduction into the guide wall. (5) Exhaust valve stem tip (*E*): This region primarily dissipates heat via solid conduction through contact with surrounding components.

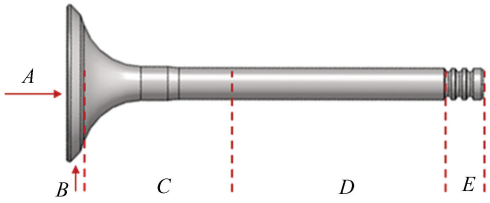

Fig.6 Thermal boundary conditions of the exhaust valve

The thermal boundary conditions for each exhaust valve region were modeled as third-type (convective) boundary conditions, and the corresponding convective heat transfer coefficients were determined using thermal resistance and forced-convection models, as listed in Table 3.

Table 3 Thermal boundary conditions of the exhaust valve

Parameters	Temperature (K)	Convective heat transfer coefficient ($W/m^2 \cdot K$)
A	873	395
B	653	5000
C	873	600
D	423	300
E	300	243

In the single-exhaust valve assembly, four contact pairs were defined as follows: (1) Exhaust valve-cam: the cam provides driving force during rotation, and the contact was modeled as frictionless; (2) Exhaust valve-exhaust valve guide: due to effective lubrication, the contact was modeled with a friction coefficient of 0.1; (3) Exhaust valve-exhaust valve seat: given the long-term high-temperature environment and the need to ensure sealing, the contact was modeled with a friction coefficient of 0.3.

During operation, the exhaust valve is primarily subjected to the spring force and the in-cylinder pressure. The boundary conditions and loading of the single-exhaust valve system were defined as follows: the cam, exhaust valve guide, and spring seat were modeled as rigid bodies to reduce computational cost, whereas the exhaust valve and exhaust valve seat were modeled as elastic bodies. The cam was set to a rotational speed of 2100 r/min; the spring was modeled between the two spring seats with a stiffness of 30000 N/m and an initial preload of 290 N. The exhaust valve guide and seat were fully constrained, and a time-dependent cylinder pressure with a peak value of approximately 22 MPa was applied to the exhaust valve head.

2 Results and Discussion

2.1 Effect of Porosity on the Properties of Bimetal

2.1.1 Effect of porosity on the tensile properties of bimetal

The GH4169/cast iron bimetal exhibited relatively high porosity, and numerous defects were observed at the interface. The porosities of the bimetals fabricated under process schemes 1, 2, 3 and 4 were 12.05%, 4.24%, 2.68% and 0.27%, respectively. Fig.7 illustrates the cross-sectional microstructures of the GH4169/cast iron bimetals. Under high porosity conditions (process scheme 1), numerous pores are present within the GH4169 region, and the pore sizes at the bimetallic interface are even larger. When the porosity is reduced to 4.24% (process scheme 2), defects within the GH4169 region decrease markedly; however, relatively large pores remain at the interface. These large interfacial defects may act as stress concentrators during loading, potentially causing premature fracture at the interface. Once the porosity decreases to a certain threshold, no apparent defects are observed in either the GH4169 region or the interfacial zone (process scheme 2).

Tensile tests were individually conducted on the three bimetal specimens with relatively high porosity (process schemes 1 – 3) under strain-controlled

loading at a rate of 2.5×10^{-4} s^{-1} until fracture at room temperature. Fig. 8 presents the stress-strain curves of tensile specimens with different porosities. Among them, the tensile strength of the specimen from process scheme 3 was the lowest, 280.66 MPa; the specimen from scheme 2 exhibited a much higher tensile strength of 463.48 MPa compared with scheme 3; and the specimen from scheme 1 achieved the highest tensile strength of 482.88 MPa. Comparison of the stress-strain curves from schemes 1 and 2 reveals that both specimens fractured at the bimetallic interface during tension, indicating that interfacial tensile strength increases as porosity decreases. When porosity was further reduced to ~2.68%, fracture occurred within the cast iron rather than at the interface, demonstrating that the interfacial strength had exceeded that of cast iron.

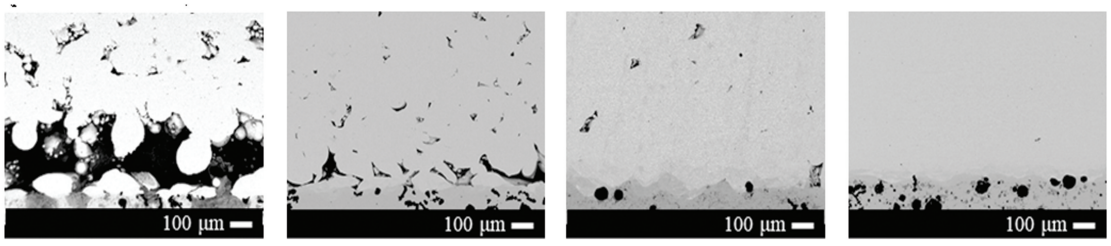

(a) Process schemes 1 (b) Process schemes 2 (c) Process schemes 3 (d) Process schemes 4

Fig.7 Cross-sectional microstructure of the GH4169/cast iron bimetal

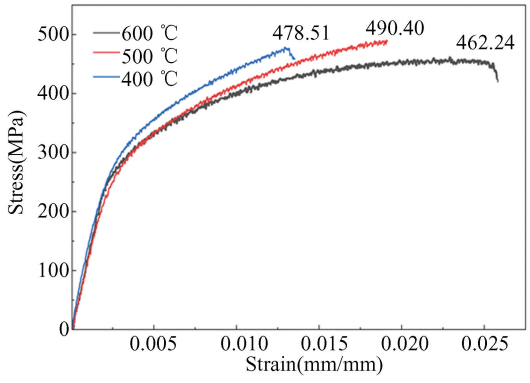

Fig. 8 Stress-strain behaviour of bimetals with varying porosity

Porosity is thus a critical factor governing the fracture behaviour of GH4169/cast iron bimetals. High porosity in the GH4169 region implies abundant interface defects that act as stress concentrators. These voids reduce the effective bearing area at the interface, making it the most vulnerable region to failure under tensile loads. As porosity decreases, interface defects are reduced, thereby improving continuity and enhancing bond quality. At low porosity levels, the effect of porosity on tensile strength becomes negligible[19], and the interface exhibits strong load-bearing capacity. At this stage, the interface no longer limits tensile performance; fracture instead occurs within the cast iron, which becomes the weakest region in the GH4169/cast iron system. Therefore, reducing porosity (i.e., increasing density) improves the metallurgical bonding quality at the interface and enhances interfacial tensile strength, allowing the overall mechanical performance of the bimetal to approach that of cast iron, the weaker constituent. Controlling porosity to a sufficiently low level ensures reliable performance; within the parameter range of this study, when porosity was reduced below 2.68%, the interfacial tensile strength of GH4169/cast iron bimetal surpassed that of cast iron.

2.1.2 Effect of porosity on the fatigue properties of bimetal

The GH4169/cast iron bimetal produced under process scheme 1 exhibited a tensile strength of only 280.66 MPa, with high interfacial porosity and poor bonding quality (as presented in Fig.7(a)); therefore, fatigue testing was not considered meaningful. Accordingly, fatigue tests were conducted on the bimetals fabricated under process schemes 2 and 3 to evaluate the influence of porosity on fatigue performance, as summarised in Table 4. For process scheme 2 (porosity 4.24%), the specimen endured approximately 186736 cycles at room temperature and 80083 at 250 ℃, with fracture consistently occurring at the bimetallic interface. In contrast, when porosity was reduced to 2.68% (process scheme 3), the specimens survived more than 1000000 cycles under room and elevated temperatures.

Table 4 Cycles of bimetals with different porosities

Process scheme	Porosity (%)	At room temperature		At 250 ℃	
		Fatigue cycles	Fracture location	Fatigue cycles	Fracture location
2	4.24	186736	Interface	80083	Interface
3	2.68	≫1000000	–	≫1000000	–

The coupled influence of porosity and temperature dictates the fatigue life of GH4169/cast iron bimetals. At a porosity of 4.24%, numerous residual voids remain at the interface (as displayed in Fig.7 (b)), acting as stress concentrators under cyclic loading and facilitating crack initiation and propagation. In this case, interfacial defects dominate the fatigue failure process, with the rate of degradation further accelerated at elevated temperatures[20]. Previous studies[21] have also shown that when the porosity of LPBF-fabricated components is reduced below a certain threshold, fatigue behaviour shifts from defect-dominated to microstructure-dominated. When the porosity decreases to 2.68%, no noticeable defects are observed at the GH4169/cast iron interface, and the interfacial metallurgical bonding quality is improved (as displayed in Fig.7 (c)). Consequently, stress concentration is effectively suppressed, with fatigue life exceeding 10^6 cycles at both room temperature and 250 ℃. Under these conditions, fatigue performance is no longer governed by interfacial defects but is instead controlled by the weaker component within the bimetal. Therefore, reducing porosity significantly enhances the fatigue resistance of GH4169/cast iron bimetals, bringing their performance closer to that of the weaker material. These findings further validate the applicability of bimetal in structural components.

2.2 Thermal and Dynamic Behaviour of Bimetallic Exhaust Valves

Under low porosity conditions, the tensile and fatigue properties of the GH4169/cast iron bimetal in high-temperature environments are mainly limited by the weaker of the two materials, which is cast iron. Compared with cast iron, GH4169, the former has worse high temperature strength, less plasticity, poorer crack resistance, and these factors reduce the service life of bimetallic parts. The temperature and mechanical load that the exhaust valve faces under service conditions affect whether it is feasible to use GH4169/cast iron bimetal.

2.2.1 Thermal behaviour of bimetallic exhaust valves

Fig.9(a) shows the thermal characteristics of the 21-4N exhaust valve in service, such as temperature, temperature gradient, and heat flux density. The valve head and neck regions encounter high-temperature gas flow, which results in a quick temperature rise. The conical seat region, in solid-to-solid contact with the exhaust valve seat, keeps the relatively low temperature. As the main heat conduction pathway, the valve stem is in the lowest temperature environment.

Fig.9 (a) shows that the distribution of the heat-flux density in the exhaust valve indicates the path of heat transfer. Heat within an exhaust valve is mostly taken away through the conical seat and the stem. Large heat flux density at the conical seat, which has heat transfer by solid-to-solid with the exhaust valve seat. The area with the greatest heat flux density is between the exhaust valve head and the valve stem, and the heat is then dissipated along the valve stem. In the exhaust valve stem, the heat flux density is radially uniform. At the exhaust valve stem, the heat flux density has a uniform radial distribution, but there is an obvious axial gradient that decreases gradually from the head to the stem tail and reaches a minimum.

Exhaust valves of different materials show the same temperature distribution pattern under service conditions, but their temperature levels and gradients vary greatly. As shown in Fig.9, the 21-4N exhaust valve, due to its relatively low thermal conductivity, has the highest temperature peak (792.6 K) and the greatest temperature gradient (2.49×10^4 K/m). The thermal conductivity of GH4169 is higher than that of 21-4N. Therefore, the GH4169 exhaust valve exhibits a lower peak temperature but the greatest temperature gradient. Of the three materials, cast iron has the highest thermal conductivity, which allows for quicker heat transfer inside the exhaust valve and lowers the peak temperatures and the temperature gradient. But it raises the lowest temperature of the valve stem as well.

The higher thermal conductivity of cast iron improves the heat dissipation capability of the GH4169/cast iron bimetallic exhaust valve. Table 5 summarizes the maximum temperature, lowest temperature, interface temperature, and highest temperature gradient of bimetallic exhaust valves at

different interface positions. The proportion of cast iron decreases as the interface position changes from 1 to 4, which leads to a 10.5 K increase in the peak temperature of the valve head, with little change in the valley temperature of the valve stem. The temperature of the interface decreases from 769.4 K to 553.9 K while the highest temperature difference is from 1.67×10^4 K/m to 2.29×10^4 K/m. As the interface approaches the valve head, a greater portion of cast iron improves heat dissipation performance and reduces the temperature gradient. However, exposure to high temperatures makes the surfaces of the interfaces and cast iron unreliable. Conversely, when the interface is located nearer to the valve stem, the higher proportion of GH4169 enhances the high-temperature mechanical performance of the exhaust valve, yet subjects the component to greater thermal loads, reducing its service life. Therefore, the interface position in GH4169/cast iron bimetallic exhaust valves should be optimized based on actual service temperatures and loads to achieve a balance among interfacial strength, long-term durability, and economic efficiency.

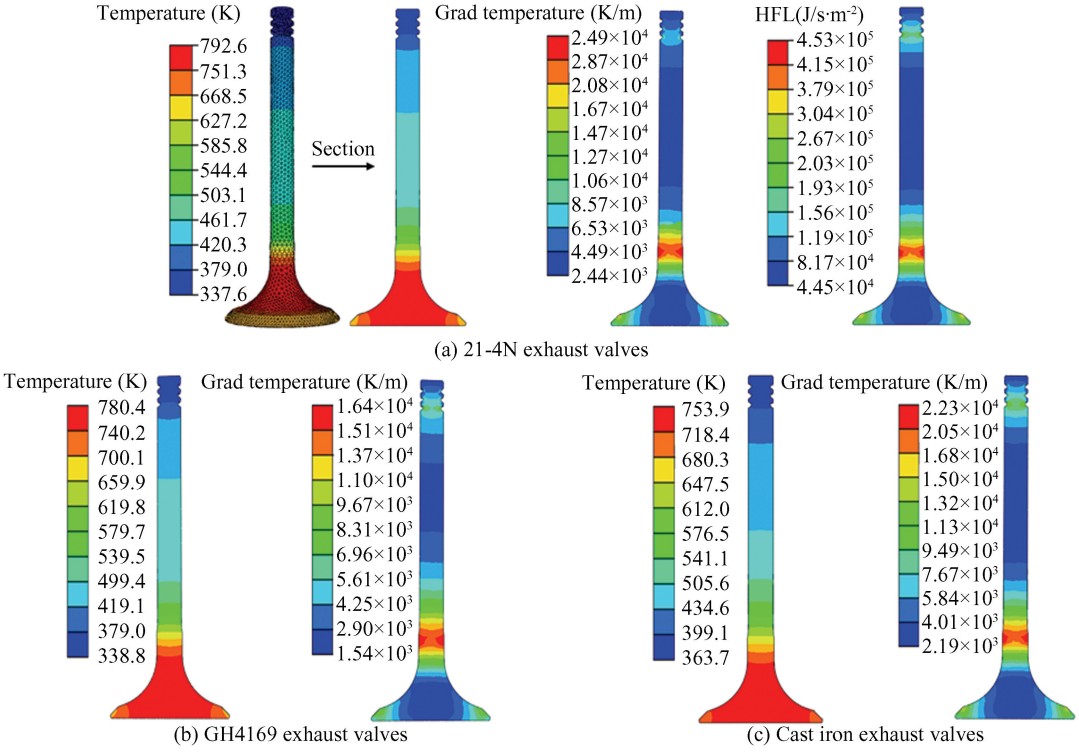

Fig.9 Thermal characteristics of exhaust valves with different materials

Table 5 Temperature of GH4169/cast iron bimetallic exhaust valves with different interface positions

Position	Temperature (K)			
	Max. temperature	Min. temperature	Interface temperature	Max. grad temperature
Position 1	769.4	328.2	769.4	1.67×10^4
Position 2	772.0	328.2	698.0	1.66×10^4
Position 3	775.2	328.1	626.2	1.97×10^4
Position 4	779.9	327.9	553.9	2.29×10^4

2.2.2 *Dynamic behaviour of bimetallic exhaust valves*

The exhaust valve returns from the fully open position to the seat under the combined action of spring force, inertial forces, and cylinder gas pressure. Fig.10 illustrates the temporal variation of spring force, valve lift, and seating velocity. The valve spring is preloaded to 290 N to ensure reliable sealing during closure. A strong coupling between valve lift and spring force is observed: as valve lift increases, the spring compresses and force rises, reaching a peak of approximately 430 N at the maximum lift (approximately 5.06 mm), thereby providing reliable

return force during closure. Valve seat closure velocity approaches −0.067 m/s while closing, and it suddenly becomes 0 when it contacts the seat instantly. When the valve is at the valve seating instant, it encounters a significant impact load, which is mainly caused by the spring and the inertia together.

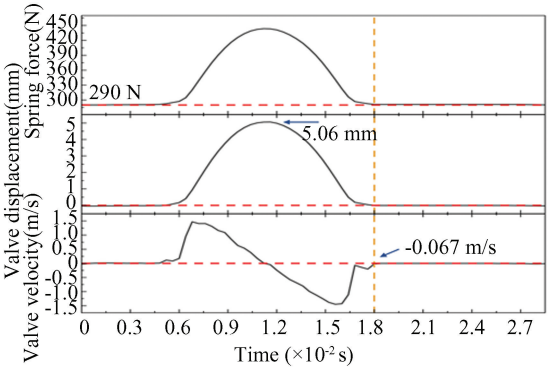

Fig.10 Valve motion characteristics

Fig.11 represents the stress distribution of the exhaust valve at various instants. Under the influence of spring preload, before the valve opens, the main stress on the valve is the axial static load generated by the spring, with low and evenly distributed stresses, and the highest stress occurs at the geometric transition between the valve head and the stem, as shown in Fig.11(a).Fig.11(b) is the stress distribution of valve seating. Combined with spring force and inertia, the valve contacts the seat, causing localized stress concentration at the seat cone. Geometric discontinuities of the valve stems serve as a point for load transfer and have a high concentration of stress. During combustion (as shown in Fig.11(c)), high-temperature, high-pressure gases are applied to the surface of the valve head, causing a peak stress in the valve surface area and reaching a maximum of 166.5 MPa. In the valve stem area, the stress is much lower, about 15.2 MPa.

The behavior of valves under dynamics is heavily dependent on their mass. Lighter materials reduce inertia and make responsiveness quicker at higher speeds. Table 6 gives the mass of the GH4169/cast iron bimetallic exhaust valve at different interface positions, along with the corresponding seat velocity and the maximum/minimum stress value. The mass difference between the GH4169/cast iron bimetal valves and the 21-4N valve is minimal. When the interface is at position 1, it is closer to the valve head and hence has the least mass for the exhaust valve. This configuration can obtain a higher closing speed and lower stress level. The remaining material has roughly the same mass, dynamics, and stress distribution. As can be seen from above, the quality of the GH4169/cast iron bimetallic exhaust valve is about the same as that of the 21-4N valve, and the effect of mass on stress distribution is very small.

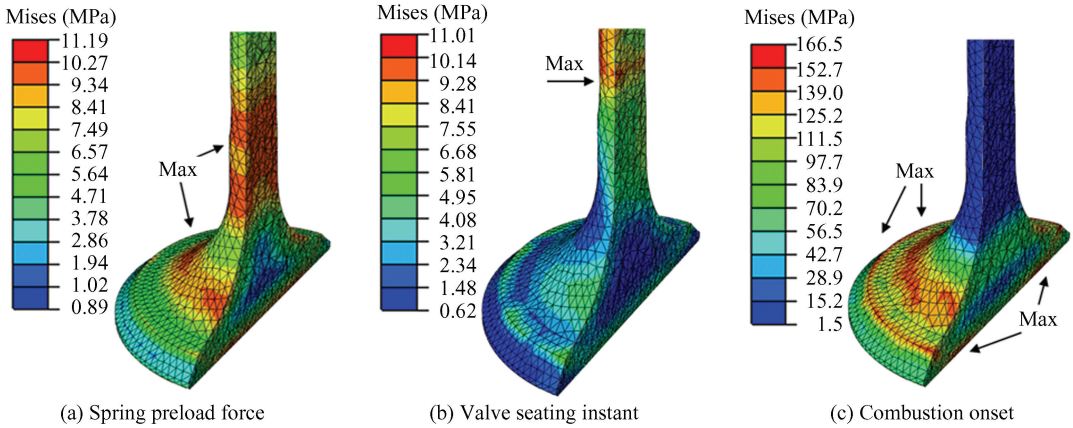

(a) Spring preload force (b) Valve seating instant (c) Combustion onset

Fig.11 Stress distribution of the exhaust valve at different operating instants

Table 6 Mass, seating velocity, and maximum/minimum stress of exhaust valves with different materials

Materials	Weight (kg)	Valve velocity (m/s)	Max. mises (MPa)	Min. mises (MPa)
21-4N	0.782	−0.014	166.5	15.20
GH4169/cast iron (Position 1)	0.766	−0.067	158.0	14.27
GH4169/cast iron (Position 4)	0.784	−0.012	169.0	18.13

2.3 Reliability of Bimetallic Exhaust Valves at Different Temperatures

GH4169/cast iron bimetallic exhaust valves are subjected to cyclic thermo-mechanical loading during service, including transient thermal shocks induced by high-temperature gas impingement, inertial impact loads generated during valve opening and closing, and contact stresses at the valve seat interface. These complex loading conditions collectively govern the long-term reliability of the component. The predominant failure mechanisms of GH4169/cast iron bimetallic valves include premature interfacial failure, low-cycle fatigue caused by repetitive seating impacts, and fatigue crack initiation and propagation within the constituent materials. Therefore, the interfacial metallurgical bonding quality and the high-temperature fatigue resistance of the bimetallic structure are critical factors determining its operational reliability.

Within the scope of the present process trials, when the porosity of the bimetal decreased to 2.68%, its tensile and fatigue properties were already governed by the weaker constituent, namely cast iron. For the bimetallic exhaust valves fabricated under process scheme 4, the porosity was as low as 0.2%. Thus, their tensile and fatigue behaviour can likewise be inferred to be cast iron dominated. Based on the simulated temperature distributions at different interface positions, 400 ℃, 500 ℃, and 600 ℃ were selected as thermal loads to test the tensile strength of the process scheme 4 bimetal.

Fig.12 presents the stress-strain curves of GH4169/cast iron bimetals fabricated under process scheme 4 at 400 ℃, 500 ℃, and 600 ℃. The measured tensile strengths at 400 ℃, 500 ℃, and 600 ℃ were 478.51 MPa, 490.40 MPa, and 462.24 MPa, respectively. All specimens fractured on the cast iron side, demonstrating that the interface possessed strong metallurgical bonding, and its strength at elevated temperature exceeded that of cast iron. With increasing temperature, both tensile strength and fracture strain declined, significantly reducing the service reliability of bimetallic exhaust valves under high-temperature operating conditions. Higher tensile strength generally suppresses crack initiation and propagation under cyclic loading, leading to higher fatigue strength. Given the extremely low porosity, the fatigue performance of this bimetal is not expected to be influenced by defect distribution. The high-temperature tensile-compressive fatigue strength of cast iron is approximately 0.3−0.55 of its tensile strength[22], which provides a basis for estimating the fatigue strength of this bimetal. By estimating fatigue strength as approximately 0.3 times the tensile strength, the fatigue strengths of GH4169/cast iron bimetals at 400 ℃, 500 ℃, and 600 ℃ were calculated to be 146.25 MPa, 147.12 MPa, and 138.67 MPa, respectively. These results are consistent with literature reports in Refs. [23 − 24], which indicate that the fatigue strength for cast irons of similar grades is about 143 − 160 MPa at 400 ℃ and 108−140 MPa at 500 ℃.

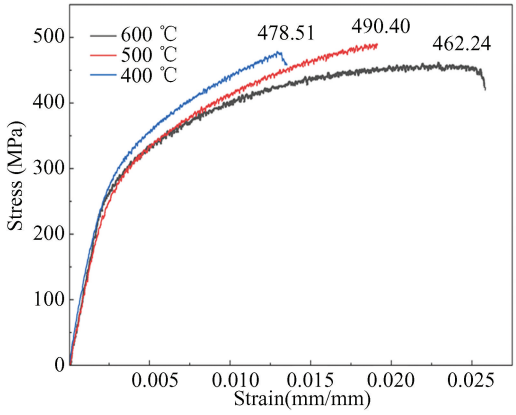

Fig. 12 Stress-strain curves of bimetals with different temperatures

Based on the simulated stress distribution, the maximum operating stress and corresponding temperature can be compared with the fatigue strength of the GH4169/cast iron bimetal at service temperatures to evaluate the safety margin of the bimetallic exhaust valve. Dynamic analysis of the exhaust valve shows that the valve stem bears stress around 15 MPa and the highest stress of the valve head reaches about 166.5 MPa, the GH4169/cast iron bimetal interface at position 1 locates in the geometric transition area of the valve head, which is under the influence of high temperature (792 K) and stress concentration (166.5 MPa) during combustion, and exceeds the fatigue strength of cast iron at 600 ℃. The temperature at the valve stem has dropped to around 500 − 700 K, and the stress is well below the fatigue limit for GH4169/cast iron bimetal at those temperatures. GH4169/cast iron bimetal interface is in a safe position at positions 2, 3, and 4. Interface position 2 is an optimal balance of quality and cost effectiveness and represents the best possible design. Moreover, a superior metallurgical bonding interface forms under low porosity, thereby suppressing crack

initiation and delamination during thermal cycling.

From a design margin and a service life standpoint, GH4169 used in the high-temperature area improves the high-temperature strength and fatigue resistance of the exhaust valve; cast iron used in the low-temperature area is a compromise between excellent thermal conductivity and cost-effectiveness. Based on thermal stress distribution, interface temperature, and dynamic mechanical load, the GH4169 cast iron bimetallic exhaust valve has very good reliability under general working conditions, which can meet the long-term working requirements of the engine exhaust system.

3 Conclusions

By controlling porosity and adjusting interface positions, the LPBF-fabricated GH4169/cast iron bimetallic exhaust valve demonstrates reliable operation under service conditions, which gives a feasible design approach to apply bimetallic valve components in engineering. The main conclusions are as follows.

1) Porosity is the main factor that controls the mechanical behavior at the GH4169/cast iron bimetallic interface. High porosity greatly decreases the interface tensile strength and fatigue life, leading to premature interface failure. Porosity is less than about 2.67 % where the interfacial tensile strength exceeds that of the cast iron, and the fatigue life is more than 10^6 cycles, so that the overall mechanical behavior is essentially that of the cast iron.

2) Exhaust valve thermal behavior is affected by both material thermal conductivity and geometric structure. The valve head region has the highest temperature; the valve stem and valve seat cone are the main heat-dissipation paths. The increase of the cast iron ratio in the bimetallic exhaust valve improves thermal conductivity and decreases temperature gradients, improving thermal stability. Substantial stress gradients arise when a valve is working. Peak stresses (166.5 MPa) occur at the geometric discontinuity between the valve head and the valve seat cone, while stem stresses remain consistently lower (15 MPa). Hence, the bimetallic interface must be placed to avoid exposure of the cast iron to high temperature and high stress regions.

3) GH4169/cast iron bimetal with low porosity (0.2%) has excellent high temperature mechanical properties. Within 400-600 ℃, it is much more than the loads the valves face, so it is quite reliable for exhaust valves. When the interface is at position 2, the GH4169/cast iron bimetallic exhaust valve has the best combination of performance and cost.

Conflict of interest: The authors declare that they have no conflict of interest regarding the publication of this article.

References

[1] Tomaszewski S, Grygier D, Dziubek M. Assessment of engine exhaust valve materials. Combustion Engines, 2023, 194(3): 48-51. DOI: 10.19206/CE-166569.

[2] Mascarenhas L A B, De Oliveira Gomes J, Beal V E, et al. Design and operation of a high temperature wear test apparatus for automotive exhaust valve materials. Wear, 2015, 342-343: 129-137. DOI: 10.1016/j.wear.2015.08.017.

[3] Luo C Z, Zeng X X, Yao Y J, et al. Fracture failure analysis and improvement of engine exhaust valve. Heat Treatment of Metals, 2024, 49(12): 301-305. DOI: 10.13251/j.issn.0254-6051.2024.12.048.

[4] Huang G F, Li D, Xu D S, et al. Failure analysis of impact fatigue fracture of 23-8N valve. Mechanical & Electrical Engineering Technology, 2024, 53(9): 227-231. DOI: 10.3969/j.issn.1009-9492.2024.09.047.

[5] Xu D S, Li C Y, Yuan Z R, et al. Fault analysis and optimization design of cone ring of exhaust valve on a diesel engine. Internal Combustion Engines, 2022, 38(5): 34-39. DOI: 10.3969/j.issn.1000-6494.2022.05.007.

[6] Vladimirova Y O, Shalunov E P. Development of copper dispersion-strengthened composite material with increased indexes of high-temperature strength and wear resistance for thermally loaded friction pairs. Journal of Physics: Conference Series, 2020, 1431(1): 012012. DOI: 10.1088/1742-6596/1431/1/012012.

[7] Anitha P, Majumder M C, Saravanan V, et al. Effect of burn-off length for friction welded dissimilar joints of Inconel 718 and SS410. Journal of Advances in Mechanical Engineering and Science, 2018, 4(1): 30-37. DOI: 10.18831/james.in.2018011003.

[8] Uzkut M, Ünlü B S, Akdağ M. Determination of optimum welding parameters in connecting high alloyed X53CrMnNiN219 and X45CrSi93 steels by friction welding. Bulletin of Materials Science, 2011, 34(4): article number 815. DOI: 10.1007/s12034-011-0200-7.

[9] Patel J, Mawandiya B K, Patel K, et al. Experimental investigations and effect of parameters on friction welded AISI 304 and Invar alloys. Advances in Materials and Processing Technologies, 2023, 10(4): 3280-3291. DOI: 10.1080/2374068X.2023.2233855.

[10] Li Z Y, Xu D S, Wang F H, et al. Failure analysis of

friction welded joint of engine exhaust valve. Mechanical & Electrical Engineering Technology, 2019, 48(3): 176-178. DOI: 10.3969/j.issn.1009-9492.2019.03.054.

[11] Mahmud A, Ayers N, Huynh T, et al. Additive manufacturing of SS316L/IN718 bimetallic structure via laser powder bed fusion. Materials, 2023, 16(19): 6527. DOI: 10.3390/ma16196527.

[12] Lu X D, Du J H, Deng Q. High temperature structure stability of GH4169 superalloy. Materials Science and Engineering: A, 2013, 559: 623-628. DOI: 10.1016/j.msea.2012.09.001.

[13] Khan M I, Khan M A, Shakoor A. A failure analysis of the exhaust valve from a heavy-duty natural gas engine. Engineering Failure Analysis, 2018, 85: 77-88. DOI: 10.1016/j.engfailanal.2017.12.001.

[14] Zhang M X, Pang J C, Meng L J, et al. Study on thermal fatigue behaviors of two kinds of vermicular graphite cast irons. Materials Science and Engineering: A, 2021, 814: 141212. DOI: 10.1016/j.msea.2021.141212.

[15] Seralathan S, Raju T N, Venkat I G, et al. Thermal analysis on different exhaust valve materials of compression ignition engine. Materials Today: Proceedings, 2020, 33(Part 7): 4105-4111. DOI: /10.1016/j.matpr.2020.06.550.

[16] Cerdoun M, Khalfallah S, Beniaiche A, et al. Investigations on the heat transfer within intake and exhaust valves at various engine speeds. International Journal of Heat and Mass Transfer, 2020, 147: 119005. DOI: 10.1016/j.ijheatmasstransfer.2019.119005.

[17] Zhang L, Liu L, Zhu X, et al. An electric load simulator for engine camless valvetrains. Applied Sciences, 2019, 9(8): 1591. DOI: 10.3390/app9081591.

[18] Fu Y X, Liu J X, Huang W Q, et al. Formation mechanisms of defects in additively manufactured GH4169/cast iron bimetal via a multi physics coupling model. Journal of Manufacturing Processes, 2025, 152: 805-815. DOI: 10.1016/j.jmapro.2025.08.008.

[19] Kan W H, Chiu L N S, Lim C V S, et al. A critical review on the effects of process-induced porosity on the mechanical properties of alloys fabricated by laser powder bed fusion. Journal of Materials Science, 2022, 57: 9818-9865. DOI: 10.1007/s10853-022-06990-7.

[20] AI-Maharma A Y, Patil S P, Markert B. Effects of porosity on the mechanical properties of additively manufactured components: a critical review. Materials Research Express, 2020, 7: 122001. DOI 10.1088/2053-1591/abcc5d.

[21] Cao Y F, Moumni Z, Zhu J H, et al. Effect of scanning speed on fatigue behavior of 316L stainless steel fabricated by laser powder bed fusion. Journal of Materials Processing Technology, 2023, 319: 118043. DOI: 10.1016/j.jmatprotec.2023.118043.

[22] Osakue E E, Anetor L. Estimating beam strength of metallic gear materials. FME Transactions, 2022, 50(4): 587-606. DOI: 10.5937/fme2204587O.

[23] Zou C L, Pang J C, Zhang M X, et al. The high cycle fatigue, deformation and fracture of compacted graphite iron: influence of temperature. Materials Science and Engineering: A, 2018, 724: 606-615. DOI: 10.1016/j.msea.2018.01.025.

[24] Zhang M X, Pang J C, Meng L J, et al. Study on high-cycle fatigue fracture mechanism and strength prediction of RuT450. Materials Science and Engineering: A, 2021, 821: 141599. DOI: 10.1016/j.msea.2021.141599.